Citation: Molecular Therapy — Methods & Clinical Development (2014) **1,** 7; doi:10.1038/mtm.2013.7

www.nature.com/mtm

ARTICLE

Intrathecal administration of IGF-I by AAVrh10 improves sensory and motor deficits in a mouse model of diabetic neuropathy

Judit Homs[1], Gemma Pagès[1], Lorena Ariza[1], Caty Casas[2,3], Miguel Chillón[1,4], Xavier Navarro[2,3] and Assumpció Bosch[1]

Different adeno-associated virus (AAV) serotypes efficiently transduce neurons from central and peripheral nervous systems through various administration routes. Direct administration of the vectors to the cerebrospinal fluid (CSF) could be an efficient and safe strategy. Here, we show that lumbar puncture of a nonhuman AAV leads to wide and stable distribution of the vector along the spinal cord in adult mice. AAVrh10 efficiently and specifically infects neurons, both in dorsal root ganglia (60% total sensory neurons) and in the spinal cord (up to one-third of α-motor neurons). As a proof of concept, we demonstrate the efficacy of AAVrh10 in a mouse model of diabetic neuropathy, in which intrathecal delivery of the vector coding for insulin-like growth factor (IGF-I) favored the release of the therapeutic protein into the CSF through its expression by sensory and motor neurons. IGF-I–treated diabetic animals showed increased vascular endothelial growth factor expression, activation of Akt/PI3K pathway, and stimulated nerve regeneration and myelination in injured limbs. Moreover, we achieved restoration of nerve conduction velocities in both sensory and motor nerves by AAVrh10, whereas we reached only sensory nerve improvement with AAV1. Our results indicate that intrathecal injection of AAVrh10 is a promising tool to design gene therapy approaches for sensorimotor diseases.

Molecular Therapy — Methods & Clinical Development (2014) **1**, 7; doi:10.1038/mtm.2013.7; published online 15 January 2014

INTRODUCTION

The complications of diabetes represent the main volume in disability, reduced life expectancy, and economic cost associated with diabetes.[1] The most common and debilitating complication of diabetes is diabetic peripheral neuropathy (DPN), which affects 60–70% of patients and causes frequent hospitalization in diabetes.[2] Sensorimotor polyneuropathy is the most common form of DPN and can affect all types of nerve fibers. Abnormal sensory perception in diabetic patients includes loss of pain and temperature sensation, and burning skin and tenderness, initially affecting the feet and lower legs and later hands and arms. In more advanced stages, foot ulcers and neuropathic deformities may develop, eventually resulting in 40% of nontraumatic limb amputations. Axonal degeneration, nerve fiber loss, segmental demyelination, and remyelination are characteristic pathological features of human DPN.[3] Although intensive insulin therapy to control blood glucose reduces the incidence of new clinically detected neuropathy, diabetic patients still develop DPN.

Gene therapy strategies for treatment of chronic pain, genetic and acquired peripheral neuropathies like DPN, or accelerating peripheral nerve regeneration could be envisaged if efficient gene transfer to the peripheral nervous system (PNS) would be achieved. Viral vectors offer the possibility to specifically target different cell types in the PNS. We and others have demonstrated transduction of mouse and human Schwann cells in vitro[4] and in vivo in animal models of peripheral nerve trauma.[5,6] Herpes simplex virus–based vectors were shown to efficiently transduce sensory neurons when injected subcutaneously in animal models, which has lead to the initiation of a phase 1 clinical trial for pain treatment (for review, see ref. 7). Several serotypes of adeno-associated viruses (AAV) also infect sensory neurons in the dorsal root ganglia (DRG) through direct administration into the cerebrospinal fluid (CSF), via retrograde transport or by intravenous administration.[8–12]

Among the different AAV serotypes tested, AAVrh10, a nonhuman primate serotype, was proven to efficiently transduce neurons in the brain after intracranial administration, enabling a widespread diffusion, similar to AAV1 or AAV9.[13,14] Moreover, intravenous administration of AAVrh10 in neonatal mice crosses the blood–brain barrier and drives one of the most efficient transduction to the spinal cord and central nervous system compared to other AAV serotypes.[15,16]

With the aim to study if AAVrh10 vector is capable to efficiently deliver a therapeutic gene to sensory and motor neurons, we tested the biodistribution of this vector and compared it with AAV1, AAV2, and AAV8, following intraneural and intrathecal administration in adult mice. Here, we demonstrate that after lumbar delivery of the vectors into the CSF, the AAV vectors were widely distributed to

[1]Department of Biochemistry and Molecular Biology, Center of Animal Biotechnology and Gene Therapy (CBATEG), Universitat Autònoma de Barcelona, Bellaterra, Barcelona, Spain; [2]Department of Cell Biology, Physiology and Immunology, Institute of Neurosciences, Universitat Autònoma de Barcelona, Bellaterra, Barcelona, Spain; [3]Centro de Investigación Biomédica en Red sobre Enfermedades Neurodegenerativas (CIBERNED), Instituto de Salud Carlos III, Spain; [4]Institut Català de Recerca i Estudis Avançats (ICREA), Barcelona, Spain. Correspondence: A Bosch (assumpcio.bosch@uab.es)
Received 6 November 2013; revised; accepted 7 November 2013;

the entire spinal cord, from lumbar to cervical segments. AAVrh10 efficiently infected neurons, both in DRG (near 60% of total sensory neurons) and in the spinal cord (up to 30% of motoneurons), while AAV1 was only able to transduce sensory neurons in the DRG. Finally, as a proof of concept, we demonstrated the efficiency of AAVrh10 in a mouse model of experimental diabetes, in which intrathecal delivery of AAVrh10 coding for insulin-like growth factor (IGF-I) was able to release the therapeutic protein into the CSF. In sensory and motor neurons of diabetic animals overexpressing IGF-I, we detected overexpression of vascular endothelial growth factor (VEGF) and activation of Akt/PI3K pathway as well as nerve regeneration and myelination in injured limbs. Moreover, we found increased nerve conduction velocity (NCV) in both sensory and motor nerves by AAVrh10-driven expression of IGF-I compared to green fluorescent protein (GFP)–treated mice, whereas only sensory nerve improvement was found using AAV1. These data demonstrate the potential of AAVrh10 for sensorimotor gene therapy.

RESULTS

AAVrh10 efficiently transduces sensory neurons in DRG

As a first approach to test AAVrh10 efficacy transducing sensory neurons, we delivered 1×10^{11} viral genomes (vg) into the CSF by lumbar puncture in the subarachnoid space, and it was compared to AAV1, AAV2, and AAV8. Animals were euthanized 3 weeks after administration, DRG sectioned, and GFP was quantified by direct fluorescent imaging. No transduction was obtained using AAV8, very small numbers of GFP-positive cells were counted with AAV2 (not shown), and the highest levels were achieved using AAV1 or AAVrh10. AAVrh10 tropism was characterized after intrathecal administration in the lumbar area by immunohistochemistry to specific neuronal markers. We quantified 13 ± 1.3% of transduced large neurons (NF-200 positive, Figure 1a–c) and 60 ± 3.2% of peripherin immunoreactivity (Figure 1d–f), showing GFP expression in lumbar ganglia (n = 3). Peripherin-positive neurons can be divided in calcitonin gene-related peptide or Ib4-positive nerons. Here, 29 ± 2.3% of calcitonin gene-related peptide positive colocalized with GFP (Figure 1g–i) and 11 ± 1.6% of IB4 neurons were also GFP positive (Figure 1j–l; n = 3). AAV1 transduced both large and small neurons but to a lower extent, and numbers were not quantified (Supplementary Figure S1a–f).

Although viral vectors were administered between the third and fourth lumbar vertebrae, once delivered in the intrathecal space, the virus was diluted in the CSF and could reach more proximal segments. Thus, we quantified GFP-expressing sensory neurons in lumbar, thoracic, and cervical DRG at week 1, 3, and 6 after virus administration (Figure 2a; Supplementary Figure S2). For AAV1, we detected stable transduction up to 6 weeks after injection only in lumbar DRG (Supplementary Figure S2; n = 3/time point). For AAVrh10, the highest level of transduction in the DRG was achieved at the injection area, that is the lumbar ganglia, where 56.9 ± 14.8% (n = 3 animals) of total DRG neurons showed GFP expression at 6 weeks (Figure 2a). Moderately lower levels of expression, although not significantly different, were quantified in the cervical area (36.1 ± 13.5%; n = 3 animals). However, in the thoracic segments, significantly lower numbers were detected, particularly 1 and 3 weeks after treatment, a phenomenon already described for AAV6.[10] AAVrh10-driven GFP expression was also evident along the axons of the transduced animals. Transversal sections of sciatic nerves showed around 50% of nerve fibers expressing GFP (Supplementary Figure S3a; n = 3 animals) that probably correspond to axons from infected nuclear bodies projecting to the hind limb. Moreover, direct intrasciatic injection

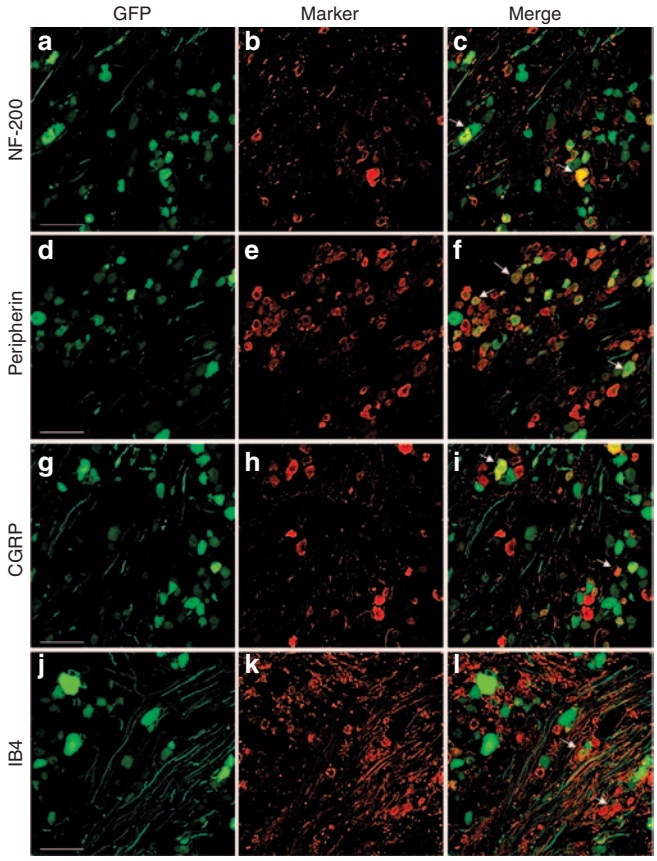

Figure 1 AAVrh10 transduction of dorsal root ganglia. (**a, d, g, j**) DRG sections from animals transduced with AAVrh10-GFP and euthanized at 3 weeks. (**b, e, h, k**) Immunohistochemistry with broad and specific markers of sensory neurons: (**b**) NF-200, (**e**) peripherin, (**h**) CGRP, and (**k**) IB4. GFP-positive sensory neurons merged with specific sensory markers (arrows, **c, f, i, l**). Scale bar = 81 µm. AAV, adeno-associated virus; DRG, dorsal root ganglia; GFP, green fluorescent protein.

of 9×10^{9} viral genomes of AAVrh10 coding for GFP targeted exclusively neurons and demonstrated its ability to be retrogradely transported to the neuronal bodies in the DRG (Supplementary Figure S3b; n = animals), as we have previously reported for AAV1 and AAV2 (ref. 6).

Intrathecal administration of AAVrh10 allows motor neuron transduction

Transduction of motor neuron after intrathecal administration of AAV9 was reported previously in mice, pigs, and nonhuman primates.[17–20] In lumbar spinal cord sections of AAVrh10-injected animals, we also observed widespread GFP expression in both dorsal and ventral areas (Supplementary Figure S4). In the white matter, we observed punctate signals, corresponding to the dorsal and ventral afferences entering the spinal cord (Supplementary Figure S4), but most importantly, at the dorsal and ventral gray matter, we also found cell bodies expressing GFP with a neuronal pattern (Figure 3). Immunohistochemical analysis with selective markers allowed us to characterize the transduced cell types. We did not detect transduction of astrocytes (glial fibrillary acidic protein–positive cells; Figure 3d–f,n) and microglia (Iba1 immunoreactivity; Figure 3j–l,p) and only very few oligodendrocytes (APC1-positive cells; Figure 3g–i,o and arrowhead in i). GFP-positive cell bodies colocalized mainly with choline acetyltransferase immunostaining, a specific

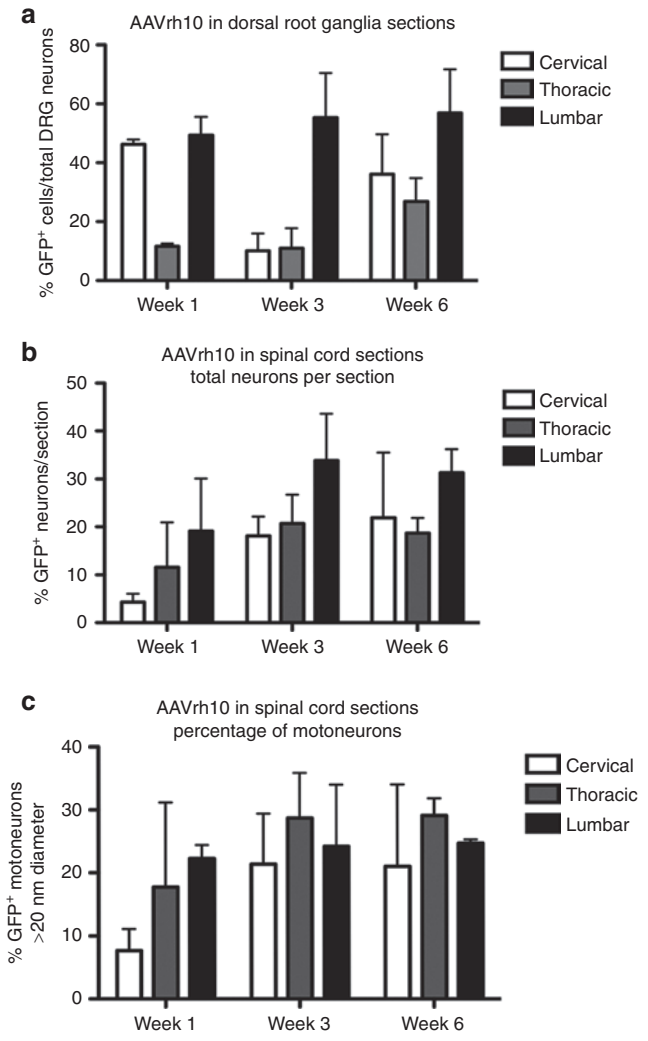

Figure 2 Quantification of GFP-positive sensory and motor neurons transduced by intrathecal AAVrh10. (**a**) Percentage of GFP-positive DRG neurons at different levels (lumbar, thoracic, and cervical) at 1, 3, and 6 weeks postinjection. (**b**) Number of GFP-positive neurons per section quantified at different segments of the ventral spinal cord (lumbar, thoracic, and cervical) after Nissl-positive colocalization. (**c**) Percentage of GFP-positive α-motoneurons quantified from **b** by size (>20 µm). Values are represented as the mean ± SEM ($n = 3$/group and time point). Statistically significant differences were observed by two-way ANOVA and Bonferroni *post hoc* tests in **a** ($P < 0.05$) at week 3 for lumbar versus thoracic and cervical numbers but not in **b** or **c**. AAV, adeno-associated virus; ANOVA, analysis of variance; DRG, dorsal root ganglia; GFP, green fluorescent protein.

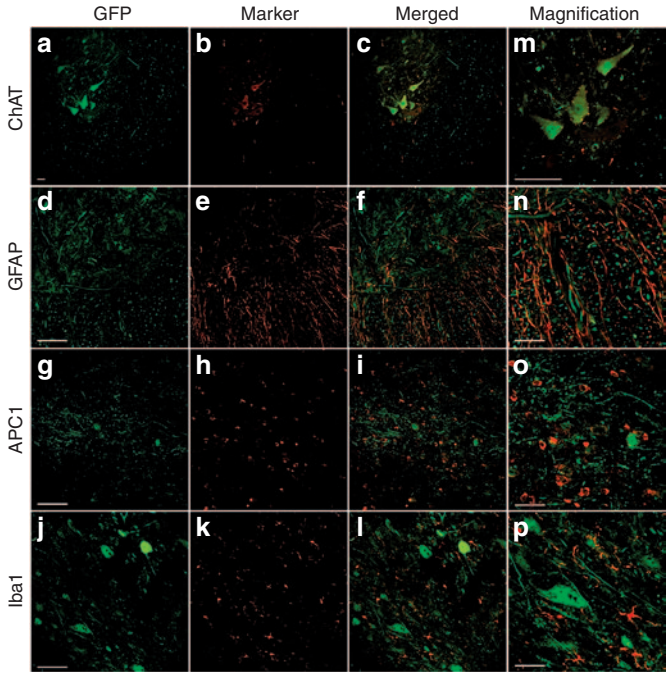

Figure 3 Tropism characterization of AAVrh10 in spinal cord after intrathecal administration of the vector. (**a, d, g, j**) GFP-transduced cells in the ventral horn of lumbar spinal cord (given in green). (**b, e, h, k**) Immunohistochemical analysis of spinal cord cross-sections with specific cell markers, (**b**) ChAT for motoneurons; (**e**) GFAP for astrocytes; (**h**) APC1 for oligodendrocytes; and (**k**) Iba1 for microglia (all given in red). (**c**) Merged images (**c, f, i, l**) showed restricted colocalization only between GFP and ChAT (**m**), except for one cell in **i** (arrowhead) colocalizing between APC1 and GFP. **a**–**l**, bar = 70 µm. Magnified merged images (**m, n, o, p**; scale bar = 31 µm). AAV, adeno-associated virus; ChAT, choline acetyltransferase; DRG, dorsal root ganglia; GFAP, glial fibrillary acidic protein; GFP, green fluorescent protein.

marker for cholinergic neurons (Figure 3a–c,m). We observed the strongest GFP signal in somatic motoneurons located in the ventral horn, of either big (>20 µm) or small size (<20 µm), and in either the medial or the lateral motor columns that send their axons to axial and limb muscles, respectively. Minor expression was detected in autonomic neurons located in the intermediolateral column in lamina VII at thoracic levels. We quantified the number of neurons in the ventral area of the spinal cord along the different spinal segments (cervical, thoracic, and lumbar; Figure 2b; $n = 3$ animals). At 3 weeks, we found near 40 neurons per section in the lumbar segments and around 20 neuronal somas in the thoracic and cervical segments without using immunohistochemistry against GFP. Importantly, one-third of α-motoneurons were transduced in all segments analyzed (Figure 2c). This demonstrates that AAVrh10-driven expression is stable over this period of time and that viruses diluted in the CSF were able to transduce sensory and spinal motor neurons in all the subdivisions of the spinal cord. Small interneurons expressing GFP as well as dorsal horn neurons were also observed, mainly in the lumbar region. Contrary to AAVrh10, AAV1-injected animals did not show GFP expression in the spinal cord (data not shown). In addition, we did not detect transduction of the meninges with any of the viruses used.

Motor and sensory neuron overexpression of IGF-I in a mouse model of DPN

As a proof of principle to test for the efficacy of AAVrh10 in treating diseases affecting both sensory and motor neurons, we used a mouse model of diabetic neuropathy by combining induction of diabetes by multiple low doses of streptozotocin with sciatic nerve crush. Four weeks after initiation of diabetes, male CD-1 mice were intrathecally injected with 1×10^{11} viral genomes of AAVrh10 or AAV1 coding for either IGF-I or GFP and submitted to sciatic nerve lesion on one leg to evaluate the regeneration delay that has been described in diabetic mice.[21,22] Electrophysiological studies were performed at 3 and 4 weeks postcrush (7 and 8 weeks after streptozotocin treatment) after which the animals were euthanized and samples processed for molecular analyses. Animals were monitored for weight and glycemia every 2 weeks (Supplementary Figure S5). All mice showed established hyperglycemia on the day of surgery without significant changes along the duration of the experiment (Supplementary Figure S5b,d). No statistically significant differences were observed between the four groups in body weight (Supplementary Figure S5a,c; Student's

t-test, $n = 10$ for GFP and 15 for IGF-I in AAVrh10-treated groups; $n = 7$ for GFP and 17 for IGF-I in AAV1-treated groups).

Electrophysiological studies showed evidences of peripheral neuropathy in the left intact hind limb of the diabetic mice that had significantly reduced motor and sensory NCV with respect to values of control mice. AAV vector injection did not induce further deterioration, and AAV-GFP mice had similar neuropathy as control noninjected diabetic mice (Table 1), despite variability between groups. Mice that received a vector for IGF-I expression showed less marked deterioration of peripheral nerve function during the month of follow-up that corresponding AAV-GFP mice. Mice with AAV1-IGF-I had significantly higher distal sensory NCV, whereas mice injected with AAVrh10-IGF-I had significantly higher amplitude of the sensory compound nerve action potential and proximal sensory NCV compared with their corresponding controls with vector encoding GFP (Table 1).

Regarding the regeneration capability, all the diabetic mice had slower rate of regeneration and reinnervation of motor and sensory targets after sciatic nerve lesion than control mice, as previously reported.[22] Administration of the AAV1-IGF-I did not produce any improvement of the regenerative capability evaluated by electrophysiological and functional methods. In contrast, mice injected with AAVrh10-IGF-I showed significantly higher motor and sensory NCV at 31 days postinjury (Table 2), suggestive of faster regeneration and maturation of the injured axons.

Four weeks after AAV injection and 8 weeks after induction of diabetes, animals were euthanized. IGF-I expression was demonstrated by immunohistochemistry in lumbar DRG and spinal cord in both AAV1- and AAVrh10-injected animals (Figure 4a,d, respectively). IGF-I immunohistochemistry in DRG differs from GFP expression shown in Figure 1 because IGF-I is a secreted protein, and as IGF-I receptor is also expressed in DRG cells,[23] it can be uptaken by other nontransduced neighboring cells, showing the global image of IGF-I signal in the DRG. Quantitative real-time PCR from lumbar DRG and ventral horn spinal cord also showed significant increase of IGF-I mRNA with both vectors compared to GFP (Figure 4b; $n = 5$–7/group; $^{**}P < 0.01$ and $^{***}P < 0.005$ by one-way analysis of variance and Tukey's multiple comparison test), correlating with immunohistochemistry images. Moreover, levels of IGF-I were also detected by enzyme-linked immunosorbent assay in the CSF of treated animals at the time of sacrifice, particularly for those injected with AAVrh10 (Figure 4c; $n = 3$/group; $^{*}P < 0.05$ by Student's *t*-test). AAV1-injected animals also showed increased IGF-I in CSF but not statistically significant from GFP-treated animals (Figure 4c). Increased IGF-I in sensory neurons probably activated Akt signaling pathway, as shown by phosphorylation of Akt compared to total Akt protein levels in AAVrh10 IGF-I and but not in GFP-injected mice (Figure 5a). IGF-I is capable to activate different signaling pathways and to promote cell survival as well as to regulate the expression of different trophic factors, VEGF being one among them. VEGF has been shown to be essential for neuronal survival, and its secretion and mRNA expression in many tissues is being induced by IGF-I. In Figure 5b, we show a significant increase in VEGF protein in lumbar DRG of IGF-I–injected animals, compared to GFP-injected mice. On the other hand, growth associated protein 43 (GAP-43) is overexpressed by neurons in the process of regeneration, and it is located in the growth cones of regenerating axons. We analyzed GAP-43 in regenerating sciatic nerves from animals injected with vectors expressing IGF-I or GFP at the time of injury. We detected a significant increase in GAP-43 mRNA in DRG and GAP-43 protein in sciatic nerve, 4 weeks after AAVrh10 IGF-I treatment (Figure 6a,b, respectively), correlating with the electrophysiological results and confirming a positive effect of IGF-I in the regeneration of injured nerves in diabetes. Levels of GAP-43 mRNA were also found increased in sciatic nerves of AAV1-injected animals but at lower levels than that in AAVrh10-injected animals. AAV1-mediated GAP-43 protein was not significantly increased in these animals (Supplementary Figure S6a,b).

Schwann cells play an important role in the regeneration process of PNS after injury. In this regard, Schwann cell survival, proliferation, motility, and myelination are crucial for a proper regeneration of the injured nerve, and all these processes can be promoted by IGF-I. We detected increased levels of PNS myelin proteins: myelin protein zero (P0), PMP22, myelin basic protein, and myelin-associated glycoprotein 4 weeks after injury in IGF-I–treated sciatic nerves (Figure 6c,d; Supplementary Figure S6c,d). Quantitative PCR of myelin proteins showed strongly increased mRNA levels in AAVrh10-injected animals and a similar tendency for AAV1-treated mice, although with lower levels. Myelin protein zero, accounting for 50% of PNS myelin proteins, was ten times enhanced in AAVrh10 IGF-I–injected animals and only four times in AAV1-injected mice, both of them being statistically significant ($P < 0.05$).

DISCUSSION

The goal of this study was to analyze the potential of AAV vectors for treating DPN. Even if DPN widely affects the PNS, restricted administration to the target tissue may be crucial, avoiding the use

Table 1 Results of electrophysiological tests performed in the intact hindlimb of diabetic mice at 7 and 8 weeks after induction of diabetes (3 and 4 weeks after intrathecal injection of viral vector in the AAV groups)

Treatment	*Control (n = 10)*		*AAV1-GFP (n = 10)*		*AAV1-IGF-I (n = 21)*		*AAVrh10-GFP (n = 7)*		*AAVrh10-IGF-I (n = 15)*	
Week diabetes	7	8	7	8	7	8	7	8	7	8
Plantar muscle										
CMAP (mV)	6.7 ± 0.4	6.5 ± 0.4	6.8 ± 0.4	6.3 ± 0.4	6.4 ± 0.3	6.3 ± 0.5	6.6 ± 0.9	6.3 ± 0.6	6.3 ± 0.3	5.9 ± 0.3
MNCV (m/s)	36.4 ± 1.2	34.8 ± 1.1	33.1 ± 0.8[c]	34.1 ± 1.1	38.8 ± 1.8	36.5 ± 0.6	36.7 ± 2.2	34.7 ± 2.1	41.3 ± 2.2	42.3 ± 2.2[c]
Digital nerve										
CNAP (μV)	29.4 ± 2.4	24.1 ± 1.1	31.9 ± 3.5	26.6 ± 2.2	32.2 ± 2.3	33.5 ± 2.7[c]	29.2 ± 3.0	20.0 ± 3.1	36.3 ± 3.0	31.2 ± 2.6[b,c]
SNCVp (m/s)	36.5 ± 0.9	34.7 ± 0.9	36.9 ± 1.9	36.0 ± 1.8	39.9 ± 1.1	37.2 ± 1.0	42.6 ± 2.8[c]	39.2 ± 1.7[c]	44.1 ± 2.8[c]	46.7 ± 2.0[b,c]
SNCVd (m/s)	29.2 ± 0.7	25.9 ± 0.7	29.1 ± 0.7	24.2 ± 0.8	32.0 ± 0.6[a]	28.7 ± 0.6[a]	28.1 ± 1.4	24.8 ± 0.9	28.6 ± 0.9	26.0 ± 0.6

Data are expressed as mean ± SEM. All CMAP and CNAP amplitudes are given for nerve stimulation at the sciatic notch.
CMAP, compound muscle action potential; CNAP, compound nerve action potential; MNCV, motor nerve conduction velocity; SNCV, sensory nerve conduction velocity; -d: distal nerve segment; -p: proximal nerve segment.
$P < 0.05$ versus [a]AAV1-GFP. [b]AAVrh10-GFP. [c]Control at the same time of follow-up. ANOVA with Bonferroni *post hoc* tests.

Table 2 Results of electrophysiological tests performed in the right hindlimb of diabetic ICR mice at 7 and 8 weeks after induction of diabetes, and 3 and 4 weeks after sciatic nerve crush (w.p.i.) and intrathecal injection of viral vector

Treatment	*AAV1-GFP (n = 9)*		*AAV1-IGF-I (n = 21)*		*AAVrh10-GFP (n = 7)*		*AAVrh10-IGF-I (n = 15)*	
w.p.i.	3	4	3	4	3	4	3	4
Ant tibialis muscle								
CMAP (mV)	12.5 ± 1.5	18.2 ± 1.8	12.6 ± 1.0	21.2 ± 1.1	14.0 ± 1.0	23.1 ± 1.6	14.7 ± 1.6	23.6 ± 2.5
Plantar muscle								
CMAP (mV)	0.54 ± 0.17	1.29 ± 0.34	0.41 ± 0.05	1.24 ± 0.21	0.63 ± 0.12	1.11 ± 0.32	0.64 ± 0.12	1.18 ± 0.18
MNCV (m/s)	11.3 ± 1.2	15.4 ± 0.8	11.3 ± 1.0	17.1 ± 1.1	10.4 ± 2.1	13.7 ± 0.7	16.1 ± 1.3[a]	18.8 ± 1.2[a]
Digital nerve								
CNAP (μV)	0.78 ± 0.44	3.43 ± 1.34	0.52 ± 0.29	3.10 ± 0.76	0 ± 0	2.60 ± 1.08	0.92 ± 0.64	3.67 ± 0.78
SNCVp (m/s)	15.3 ± 3.9	15.5 ± 1.0	16.4 ± 5.0	15.4 ± 1.4	—	21.2 ± 6.1	—	23.8 ± 1.3
SNCVd (m/s)	3.7 ± 0.5	7.3 ± 0.5	4.2 ± 0.8	7.4 ± 0.5	—	6.0 ± 0.7	—	10.0 ± 1.9[a]
Pinprick score	3.3 ± 0.5	5.8 ± 0.7	2.7 ± 0.3	5.3 ± 0.4	1.0 ± 0.0	4.0 ± 0.5	1.0 ± 0.2	5.1 ± 0.5

Data are expressed as mean ± SEM. All CMAP and CNAP amplitudes are given for nerve stimulation at the sciatic notch.
$P < 0.05$ versus [a]AAVrh10-GFP at the same time of follow-up. ANOVA with Bonferroni *post hoc* tests.
ANOVA, analysis of variance; CMAP, compound muscle action potential; CNAP, compound nerve action potential; MNCV, motor nerve conduction velocity; SNCV, sensory nerve conduction velocity; -d: distal nerve segment; -p: proximal nerve segment; w.p.i.: weeks post infection.

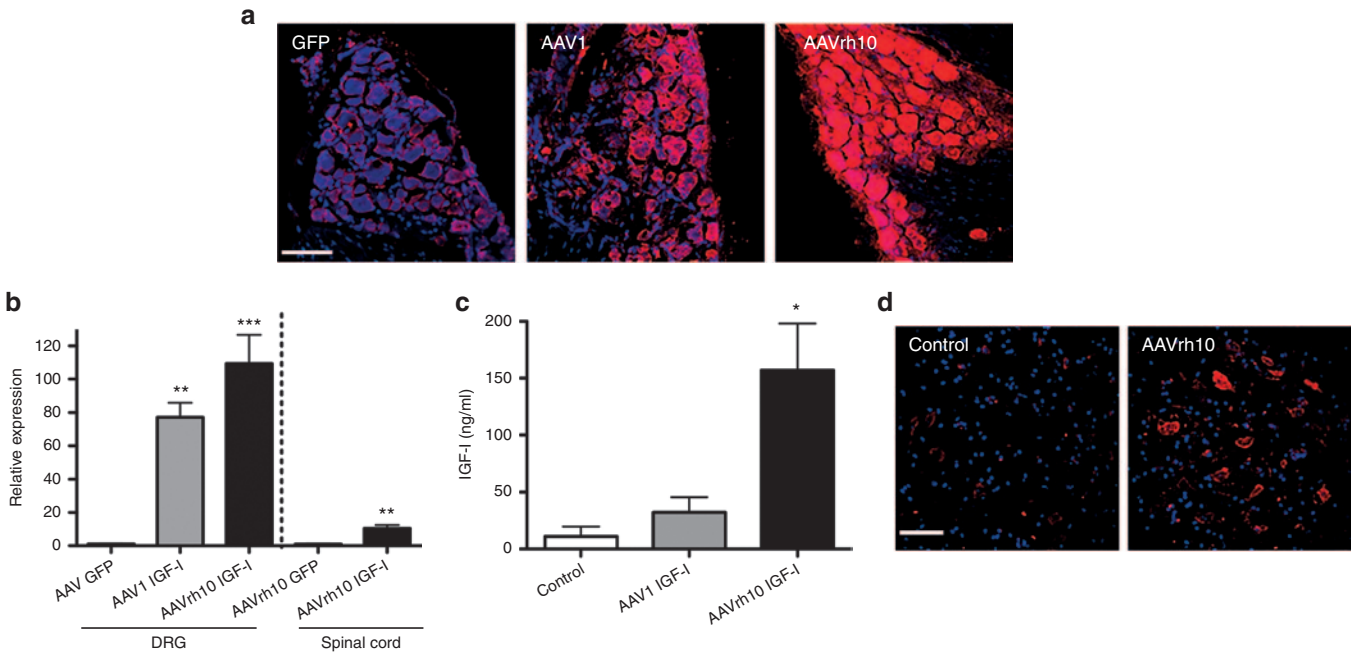

Figure 4 IGF-I expression driven by AAV1 or AAVrh10 is detected in sensory and motor neurons and secreted to the CSF of diabetic mice. IGF-I expression is demonstrated 4 weeks after intrathecal administration of AAV vectors. (**a**) IGF-I immunohistochemistry in DRG and (**d**) ventral spinal cord sections from the lumbar area. Confocal microscopy detected increased IGF-I staining in sensory and motor neuron-like morphology in mice injected with AAV1-IGF-I and AAVrh10 IGF-I compared to control animals injected AAV coding for GFP. Images were obtained sequentially under identical scanning conditions for each independent channel (red channel: IGF-I; blue channel: TO-PRO-3 to counterstain nuclei; $n = 2$). (**b**) Quantitative PCR from lumbar DRG and ventral horn of spinal cord showed significant increase of IGF-I with both vectors compared to GFP (one-way ANOVA and Tukey's multiple comparison test; $^{**}P < 0.01$; $^{***}P < 0.005$; $n = 5$–7/group). (**c**) IGF-I ELISA from CSF of treated animals obtained at the time of sacrifice ($n = 3$/group). Statistically significant numbers were obtained for AAVrh10-treated animals but not with AAV1, compared to nontreated control animals (Student's *t*-test, $^{*}P < 0.05$). **a**, bar = 160 μm **d**, bar = 73 μm. AAV, adeno-associated virus; ANOVA, analysis of variance; CSF, cerebrospinal fluid; ELISA, enzyme-linked immunosorbent assay; IGF, insulin-like growth factor.

of large doses of vector and the chance of expression of recombinant proteins in undesired tissues, leading to development of secondary effects or stimulation of the immune response against the virus or the therapeutic protein.[24,25] For this reason, we delivered AAV1 and AAVrh10 vectors to the CSF by lumbar puncture, a minimally invasive route that can be potentially performed in an outpatient setting, so to allow reaching sensory and motor neurons with minor exposure of peripheral tissues. Broad delivery to the PNS by targeting sensory and/or motor neurons is required to treat neuropathic pain, nerve trauma, or diseases-like DPN, Charcot–Marie–Tooth, amyotrophic lateral sclerosis, or spinal muscular atrophy.[26–28] Here, we demonstrate that AAVrh10 delivered by

lumbar puncture infects both sensory and motor neurons along the different segments of the spinal cord, with only significant differences in the relative percentage of neurons transduced between lumbar and thoracic DRG, but no differences were found between motoneurons or even between lumbar and cervical DRG. With only 10 µl of viruses, we achieved up to 60% of sensory neurons and 30% of motoneurons transduced. Moreover, in this work, we have used single-strand AAV as a platform, reported to be 20-fold less efficient compared to self-complementary AAVs, and we did not use immunohistochemistry to quantify GFP expression in transduced cells to avoid overestimation due to background, so we may have, in addition, ten times lower sensitivity when quantifying transduction levels.

Studies in larger animals are important to evaluate the potential of the therapeutic strategy. As a matter of fact, intramuscular AAV6 in nonhuman primates could target 50% motoneurons in 1-cm-long lumbar spinal cord segment.[29] Moreover, intravenous AAV9 was able to transduce motoneurons in adult cats up to 15% from lumbar to cervical segments, although peripheral tissues, including testis, were also labeled.[30] Recently, intrathecal administration of AAV9 in pigs and nonhuman primates demonstrated the capability of transducing sensory and motor neurons. However, most of transduced cells were astrocytes.[20,31,32] This is also in accordance with the preferential transduction of astrocytes after intravenous administration of this vector in adult mice.[33] Other serotypes, like AAV7, seem to be as efficient as AAV9 after intracisterna injection and targets both neurons and astrocytes.[19] Herein, we demonstrate AAVrh10-specific tropism for neurons in the spinal cord and DRG, similar to what was reported for the central nervous system,[14] but not for glial cells as found for AAV7 and AAV9, which may be an advantage because restricting cell type infection may decrease immunological response, although this needs to be analyzed.[20] In this regard, a high percentage of humans are seropositive for different AAV serotypes. In adults, anti-AAV2 antibodies are the most prevalent (up to 70% of healthy humans), followed by serotypes AAV5, AAV9, and AAV8.[34] Using a nonhuman AAV serotype in human gene therapy trials may have additional advantages compared to human serotypes like AAV9, since patients may not be preimmunized against this serotype, although cross-reaction between AAVrh10 and human AAV serotypes needs to be quantified.

As a proof of principle, we administered IGF-I as therapeutic gene in the mouse model of DPN. IGF-I provides trophic support to neurons of peripheral and central nervous systems. Through its tyrosine kinase receptor, IGF-I upregulates other neurotrophic factors including hypoxic-inducible factor 1α and VEGF.[35] Schwann cells express IGF-I receptors, and their activation promotes myelination[36] and protects Schwann cell dysfunction induced by high glucose in vitro.[37] Importantly, intrathecal daily delivery of IGF-I through an infusion pump in diabetic rats reversed slowing of motor and sensory conduction velocity as well as atrophy of myelinated sensory axons in peripheral nerve.[38] In fact, the therapeutic effect of growth factors was demonstrated for DPN by promoting neuronal survival, stimulating repair of peripheral nerve injury, or inducing nerve regeneration under diabetic conditions (for review, see ref. 39). For that reason, clinical trials using nerve growth factor, brain-derived neurotrophic factor, VEGF, and C-peptide were proposed, although without significant benefit so far.[40–43] Delivering factors continuously through gene therapy vectors may considerably improve the efficiency of these trials. Indeed, AAVrh10 vector may enable the long-term expression in sensory and motor neurons along the spinal cord without the risk of insertional mutagenesis.[44] Delivering nonsecreted proteins through this method could be an additional challenge since only those neurons expressing the transgene will be corrected.

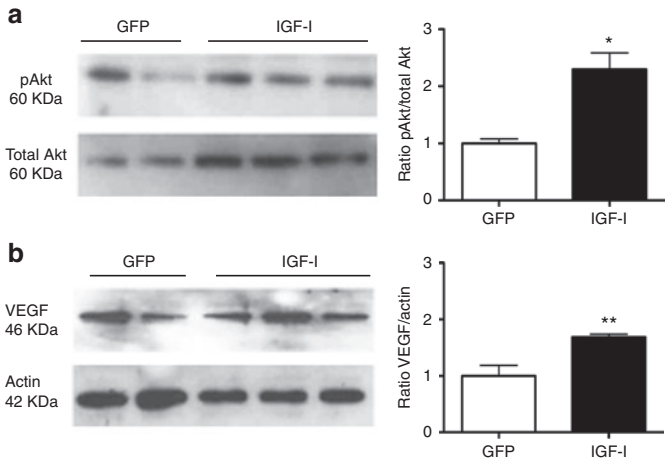

Figure 5 IGF-I signaling is enhanced in DRG of AAVrh10-treated diabetic mice. (**a**) Western blot showing phosphorylation of Ser473 Akt from DRG tissue extracts from animals injected with AAVrh10 coding for IGF-I or GFP. Total Akt was used to normalize protein levels. Western blots were scanned and represented as the ratio of phosphorylated Akt (pAkt) versus total Akt (mean ± SEM). Statistically significant differences were detected by Student's *t*-test (*$P < 0.01$; $n = 2$ for GFP; $n = 3$ for IGF-I). (**b**) DRG protein extracts were immunoblotted using anti-VEGF or actin antibodies. Densitometries show statistically significant increase of VEGF in AAVrh10IGF-I–treated DRGs (values are means ± SEM and represent ratio of VEGF normalized by actin levels from at least two blots; $n = 2$ for GFP-treated animals and $n = 5$ for IGF-I–treated animals; **$P < 0.01$ by Student's *t*-test). AAV, adeno-associated virus; DRG, dorsal root ganglia; GFP, green fluorescent protein; IGF, insulin-like growth factor; VEGF, vascular endothelial growth factor.

Unfortunately, animal models of diabetes do not reach the severity of human diabetic neuropathy. Animal nerves usually show relatively mild neurophysiological deficits and minor morphometric changes.[45,46] The lack of degenerative neuropathy in diabetic rodent models seems to be a consequence of the short life span of rodents or the physically shorter axons. Degenerative neuropathy is minimal even in larger animals like dogs or primates, with the exception of cats.[47] For this reason, we combined diabetes with nerve injury, because it is demonstrated that PNS regeneration is impaired in diabetic patients and animal models.[21,22] The results presented here demonstrate that IGF-I delivery using AAVrh10 achieves higher transduction to sensory neurons and, more importantly, to motoneurons, leading to higher levels of the therapeutic protein to both sensory and motor nerves, which is probably the cause of the higher expression of IGF-I downstream signaling pathway like myelin proteins or GAP-43 observed in our model. Altogether, these data demonstrate that IGF-I delivery through intrathecal injection to sensory neurons with AAV1 is able to achieve a modest improvement of the neuropathy but not of nerve regeneration after injury in diabetic mice, while when driven by AAVrh10, IGF-I is able to significantly accelerate regeneration and myelination of the peripheral nerve of diabetic animals, with particular effect to motor neurons. These improvements may be relevant in diabetic animal models of longer evolution, in which neuropathy is more severe, and in larger species in which axonal regeneration through longer nerves takes more time. Despite in our experimental design, we did not evaluate the effect of AAVrh10 coding for IGF-I on nerve regeneration without the effect of diabetes, our results suggest that intrathecal injection of AAVrh10 could be a promising tool to design gene therapy approaches for diseases affecting sensory and motor neurons, like DPN, as well as for peripheral nerve injury.

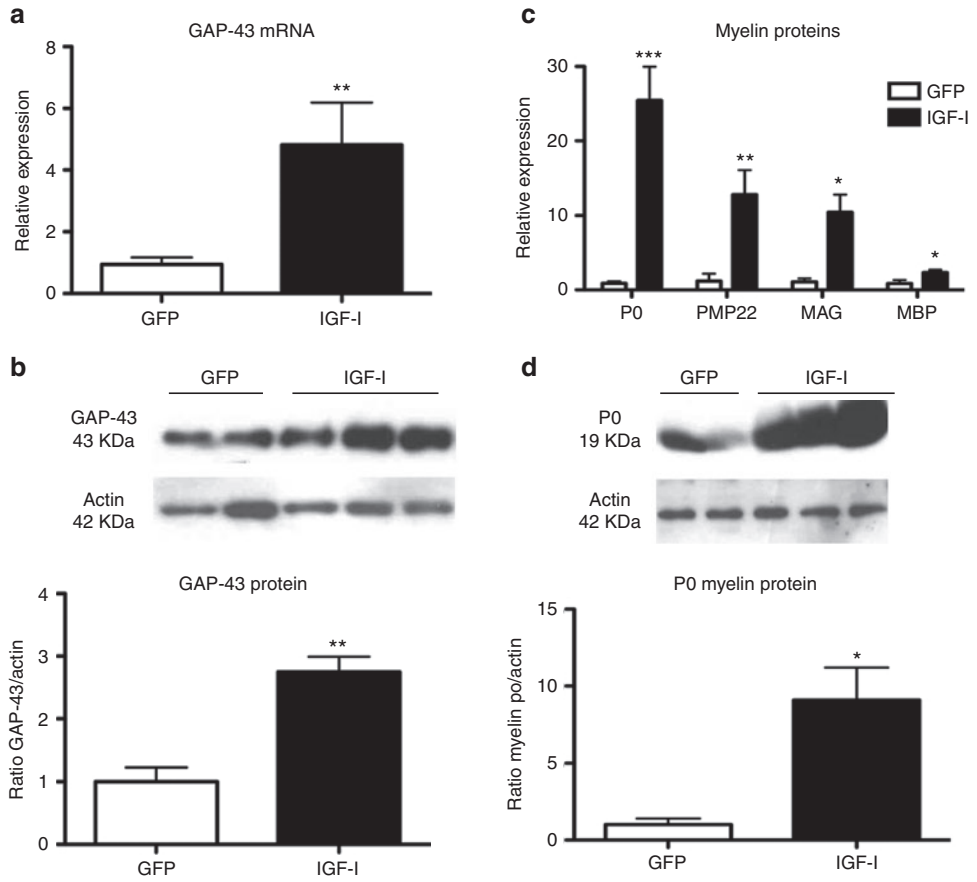

Figure 6 AAVrh10 coding for IGF-I promotes regeneration and myelin proteins expression in injured sciatic nerves of diabetic mice. Injured sciatic nerves and DRG from diabetic mice treated with AAVrh10 coding for GFP or IGF-I were dissected 4 weeks after treatment. Graphs represent means ± SEM (n = 3–5 animals). mRNA and protein of GAP-43, a marker for nerve regeneration, are significantly increased in IGF-I–treated animals as assessed by (**a**) quantitative PCR from DRG and (**b**) western blot from sciatic nerve protein extracts, where levels of GAP-43 were quantified and compared to actin. (**c**) Quantitative PCR from sciatic nerve shows increased mRNA for myelin proteins P0, PMP22, MAG, and MBP in animals that received IGF-I compared to GFP-treated mice. (**d**) Protein levels of myelin protein P0 analyzed by western blot corroborated quantitative PCR results. Student's t-tests show statistically significant results (***$P < 0.005$; **$P < 0.01$; *$P < 0.05$). AAV, adeno-associated virus; DRG, dorsal root ganglia; GAP, growth associated protein; GFP, green fluorescent protein; IGF, insulin-like growth factor; MBP, myelin basic protein.

MATERIALS AND METHODS

AAV vector construction, production, and titration

GFP cDNA was cloned into *Hind*III and *Nhe*I sites to the plasmid pAAV-CAG-polylinker-WPRE, containing the chicken β-actin promoter with the cytomegalovirus enhancer and the woodchuck hepatitis virus responsive element (WPRE). AAV2/1 and AAV2/rh10-CAG-GFP-WPRE were generated as previously described[48] by triple transfection in HEK 293-AAV cells (Stratagene, Carlsbad, CA) with branched polyethylenimine (PEI; Sigma, St Louis, MO) with the plasmid containing the inverted terminal repeats of AAV2, the AAV helper plasmid containing Rep2 and Cap for each serotype (kindly provided by JM Wilson, University of Pennsylvania, PA, USA) and the pXX6 plasmid containing helper adenoviral genes.[49] Vectors were purified by iodixanol gradients, after benzonase treatment[48] by the Vector Production Unit at Center of Animal Biotechnology and Gene Therapy (Universitat Autònoma de Barcelona).

Animals

Eight to twelve-week-old male Hsd:ICR (CD-1) (Harlan Laboratories, Indianapolis, IN) mice were used. Mice were fed *ad libitum* with a standard diet (2018S Teklad Global; Harlan Laboratories; 17% calories from fat) and kept under a light–dark cycle of 12 hours (lights on at 8:00 AM). To induce insulin-dependent diabetes, mice were given, on 5 consecutive days, an intraperitoneal injection of 45 mg/kg body weight of streptozotocin (dissolved in 0.1 mol/l citrate buffer, pH 4.5, immediately before administration). Diabetes was assessed by measuring blood glucose levels with a Glucometer Elite (Bayer, Leverkusen, Germany). Animal care and experimental procedures were approved by the Biosafety and the Animal and Human Experimentation Ethical Committees of the Universitat Autònoma de Barcelona.

Surgical procedures

Administration of viral vectors. Animals were anesthetized by intraperitoneal injection of ketamine (10 mg/kg of body weight; Imalgene 500; Rhône-Merieux, Lyon, France) and xylazine (1 mg/kg of body weight; Rompun; Bayer). Sciatic nerve injection and injury were described previously.[6] Three microliters of viral vectors were directly injected into the sciatic nerve using a 33-gauge needle and a Hamilton syringe connected to a Micropump (Micro4; World Precision Instruments, Sarasota, FL) at a rate of 400 nl/minute. Intrathecal administration was performed at the lumbar region. After lateral spine exposure, by paravertebral muscle dissection, local anesthesia with bupivacaine 0.5% (B.Braun, Melsungen, Germany) was applied. Ten microliters of viral vectors were slowly injected into the CSF through a 33-gauge needle and a Hamilton syringe between lumbar vertebrae L3 and L4. Appropriate access to the intrathecal space was confirmed by animal's tail movement. The needle remained in place at the injection site for one additional minute after which muscle and skin were sutured.

CSF extraction. Mice were deeply anesthetized and immobilized in stereotaxic appliance. An incision was made from the occipital region of the skull to the cervical region of the spine, and the posterior neck muscles were separated to access the arachnoid at the cisterna magna. Local anesthesia with bupivacaine was applied. An aspirator tube (Sigma-Aldrich) assembled to a microcapillary pipette was used to extract the CSF. A slight pressure was made with the microcapillary pipette on the arachnoid membrane to access

the cisterna magna. Then, 5 µl of CSF per mouse were withdrawn by aspiration. Animals were euthanized just after CSF extraction.

Sciatic nerve lesion. Under anesthesia as stated above, the right sciatic nerve was exposed at the mid-thigh and subjected to a crush lesion during 30 seconds for three times in succession with a Dumont #5 (World Precision Instruments, Sarasota, FL) forceps at a constant point, 42 mm from the tip of the third digit. The wound was then sutured by layers.

Functional tests

Nerve conduction studies were performed bilaterally in the sciatic nerve at two time points, 7 and 8 weeks after induction of diabetes, corresponding to 3 and 4 weeks following the surgical lesion on the right side.[22] With animals under anesthesia (pentobarbital 40 mg/kg intraperitoneally), the nerve was stimulated percutaneously through a pair of small needle electrodes placed first at the sciatic notch and then at the ankle. Rectangular electrical pulses (Grass S88) of 0.01 ms duration were applied up to 25% above the voltage that gave a maximal response. The compound muscle action potentials were recorded from the third interosseus plantar muscle and from the tibialis anterior muscle with microneedle electrodes. Similarly, the sensory compound nerve action potential was recorded by electrodes placed at the fourth toe near the digital nerves. All evoked action potentials were displayed on a storage oscilloscope (Tektronix 420, Beaverton, OR) at settings appropriate to measure the amplitude from baseline to peak and the latency to the onset of the recorded potentials. The NCV was calculated for each segment tested; motor NCV for the sciatic notch–ankle segment and sensory NCV for the proximal segment sciatic notch–ankle and for the distal segment ankle–digit. During electrophysiological tests, the animals were placed over a warm flat steamer controlled by a hot water circulating pump, and the hindpaw skin temperature was maintained above 32 °C. To reduce variability between sets, groups of mice receiving each AAV vector encoding for GFP and IGF-1 were studied in parallel and compared.

Quantitative real-time PCR

Sciatic nerves, DRG, and spinal cord were homogenized with Qiazol (Qiagen, Hilden, Germany) to obtain total RNA. Messenger RNA was retrotranscribed to cDNA (Omniscript RT Kit; Qiagen), and analysis of expression was performed by quantitative real-time PCR (Smart Cycler II; Cepheid, Sunnyvale, CA) with FastStart Sybrgreen Master (Roche Diagnostics, Basel, Switzerland). Primer sequences used: reference gene m36B4 (forward: ATGGGTACAAGCGCGTCCTG; reverse: AGCCGCAAATGCAGATGGAT); IGF-I (forward: GGACCAGAGACCCTTTGCGG; reverse: GTGCCCTCCGAATGCTGG AG); P0 (forward: TCTCAGGTCACGCTCTATGTC; reverse: CAGGTAGAAGAG CAACAGCAG); PMP22 (forward: CTCTTGTTGGGGATCCTGTTC; reverse: AA GGCGGATGTGGTACAGTTC); myelin basic protein (forward: GGTGCGCCC AAGCGGGGC; reverse: ACTTCTGGGGCAGGGAGCC); myelin-associated glycoprotein (forward: AGCACAGCGTCCTGGACATC; reverse: GGCCCAGCC AGCTCAGCTC); and GAP-43 (forward: AGCCTAAACAAGCCGATGTGCC; reverse: TTCGTCTACAGCGTCTTTCTCCTCC). Amplifications were performed as follows: heat inactivation (5 minutes, 95 °C, 1 cycle), followed by 40 cycles of 95 °C, 15 seconds; 58 °C (melting temperature for each pair of primers), 30 seconds; 72 °C, 30 seconds. Fluorescence detection of product was performed at the end of the PCR extension, and melting curves were analyzed by monitoring the continuous decrease in fluorescence of the SYBR Green signal. PCR products were verified for a single amplification product using melting curve analysis, and the molecular weight of each product was confirmed by agarose electrophoresis. Quantification relative to m36B4 controls was calculated using the Pfaffl method.[50]

Histology and immunological assays

Anesthetized animals were perfused with phosphate buffer, followed by 4% paraformaldehyde in phosphate buffer. Cryoprotected sciatic nerves, DRG, and spinal cord containing lumbar, thoracic, or cervical segments were embedded in Tissue-Tek Oct Compound (Miles, Elkhart, IN). Ten-micrometer-thick sections of sciatic nerves and DRG and 20-µm-thick sections of spinal cord and brain were blocked and incubated with primary antibodies overnight at 4 °C. For sciatic nerves and DRG, the antibodies used were: anti-PGP 9.5 (1:500; UltraClone, Isle of Wight, UK), anti-S100 (1:500; DakoCytomation, Glostrup, Denmark), anti-CRGP and anti-NF200 (1:400; Sigma-Aldrich), anti-peripherin (1:400; Millipore, Billerica, MA), and Isolectin IB4 (1:200; Millipore). Spinal cord sections were incubated with the following primary antibodies: anti-APC1 (1:400; Calbiochem, Merck KGaA, Darmstadt, Germany), anti-glial fibrillary acidic protein (1:500; DakoCytomation), anti-Iba1 (1:1,000; Wako Chemicals, Richmond, VA), anti–choline acetyltransferase (1:50; Millipore), and anti-IGF-I (1:100; Abcam, Cambridge, UK). Sections were then incubated with the following secondary antibodies: Alexa Fluor Goat Anti-rabbit 568, Alexa Fluor Goat Anti-mouse 568, and Alexa Fluor Rabit Anti-goat 568 (1:200; Invitrogen, Carlsbad, CA). Finally, sections were counterstained with Hoescht stain solution (Sigma-Aldrich) for nuclei labeling, and they were mounted in Gel Mount (Sigma-Aldrich). Fluorescence was detected with a laser-scanning confocal microscope (TCs SP2; Leica Microsystems, Heidelberg, Germany), and images taken for quantification. For DRG neuron counting, one every five sections was selected, and DRG neurons were identified as large, round cell bodies with large round nuclei, surrounded by satellite cells with small elongated nuclei, and counted by two independent researchers. At least five sections for each DRG were used. GFP was detected by direct fluorescence, without antibody enhancement.

For spinal cord neuron counting, 40 µm sections separated by 200 µm of each spinal cord were stained with Neurotrace red fluorescent Nissl (Molecular Probes, Eugene, OR) following manufacturer's instructions. GFP-positive cells localized in the ventral horn were counted, without antibody enhancement, along the spinal cord to estimate the number of ventral neurons transduced in each segment. For α-motoneuron counting, only choline acetyltransferase–positive neurons with diameters above 20 µm, with a prominent nucleolus and polygonal shape in the ventral horn were considered in Nissl-stained sections. Counting was performed by two different researchers, and data were pooled together.

Western blot. Sciatic nerves, DRGs, and spinal cord were sonicated and homogenized in RIA lysis buffer (50 mmol/l Tris–Cl pH 7.4, 150 mmol/l NaCl, 1 mmol/l ethylenediaminetetraacetic acid, 1% NP-40, and 0.25% sodium deoxycholate) and Complete Mini EDTA-free protease inhibitor cocktail tablets (Roche Diagnostics). Protein concentration was determined by BCA Protein Assay (Pierce, Rockford, IL), and 50 µg of proteins were separated on 10% sodium dodecyl sulfate–polyacrylamide gel electrophoresis gel (Bio-Rad, Hercules, CA). Polyvinylidene fluoride membranes were incubated with anti-VEGF (1:200; Abcam), anti-Akt-P (Ser473) (1:500; Cell Signaling Technology, Danvers, MA), anti-GAP-43 (1:500; Millipore) and anti-P0 (1:500; Abcam), and anti-rabbit conjugated to horseradish peroxidase (1:2,000; DakoCytomation) combined with western blotting detection reagent (ECL Plus; Amersham, Freiburg, Germany) according to the manufacturer's instructions. The same membranes were stripped and incubated with anti-actin (1:500; Sigma-Aldrich) and anti-total Akt (1:500; Cell Signaling Technology). Band pixel intensities were quantified by GeneSnap software for Gene Genius Bio Imaging System (Syngene, Cambridge, UK) and normalized by anti-actin levels in each line and by anti-total Akt levels for Akt-P samples.

Statistics

Values are represented as mean ± SEM. Statistical analyses using Student's *t*-test or one- and two-way analysis of variance with Bonferroni or Tukey *post hoc* tests were performed for each set of data. Differences were considered statistically significant if $P < 0.05$.

CONFLICT OF INTEREST

The authors declare no conflict of interest.

ACKNOWLEDGMENTS

We thank the Vector Production Unit at CBATEG (Universitat Autònoma de Barcelona) that was supported by the *Association Française contre les Myopathies* (AFM) for producing AAV vectors, James M. Wilson (University of Pennsylvania) for providing AAV1 and AAV10 RepCap plasmids, and Meritxell Puig and David Ramos (CBATEG, UAB) for technical assistance. J.H., G.P. and L.A. were recipients of predoctoral fellowships (J.H. from the AFM: AFM2008/13622AE; G.P. and L.A. from the Generalitat de Catalunya: 2009FI_B00219 and 2006FI00762, respectively). A.B. was a beneficiary of the Ramon y Cajal Program. This work was supported by the EU (Treat-NMD Network of Excellence, FP6), the Instituto de Salud Carlos III (PS09730 to A.B., ISCIII-PI10-00561 to M.C., TERCEL funds to X.N.), the Generalitat de Catalunya (SGR 2009-1300), the Marató TV3 (110432 to A.B. and C.C.) and the UAB (EME04-07).

REFERENCES

1 Whiting, DR, Guariguata, L, Weil, C and Shaw, J (2011). IDF diabetes atlas: global estimates of the prevalence of diabetes for 2011 and 2030. *Diabetes Res Clin Pract* **94**: 311–321.
2 Shaw, JE, de Courten, M, Boyko, EJ and Zimmet, PZ (1999). Impact of new diagnostic criteria for diabetes on different populations. *Diabetes Care* **22**: 762–766.
3 Dyck, P and Giannini, C (1999). Pathologic alterations in human diabetic polineuropathy. In: Dyck, P and Thomas, P (eds). *Diabetic Neuropathy, 2nd ed*. Saunders: Philadelphia. pp. 279–275.
4 Hu, Y, Leaver, SG, Plant, GW, Hendriks, WT, Niclou, SP, Verhaagen, J *et al*. (2005). Lentiviral-mediated transfer of CNTF to schwann cells within reconstructed peripheral nerve grafts enhances adult retinal ganglion cell survival and axonal regeneration. *Mol Ther* **11**: 906–915.
5 Hendriks, WT, Eggers, R, Verhaagen, J and Boer, GJ (2007). Gene transfer to the spinal cord neural scar with lentiviral vectors: predominant transgene expression in astrocytes but not in meningeal cells. *J Neurosci Res* **85**: 3041–3052.
6 Homs, J, Ariza, L, Pagès, G, Udina, E, Navarro, X, Chillón, M *et al*. (2011). Schwann cell targeting via intrasciatic injection of AAV8 as gene therapy strategy for peripheral nerve regeneration. *Gene Ther* **18**: 622–630.
7 Srinivasan, R, Fink, DJ and Glorioso, JC (2008). HSV vectors for gene therapy of chronic pain. *Curr Opin Mol Ther* **10**: 449–455.
8 Hollis, ER 2nd, Kadoya, K, Hirsch, M, Samulski, RJ and Tuszynski, MH (2008). Efficient retrograde neuronal transduction utilizing self-complementary AAV1. *Mol Ther* **16**: 296–301.
9 Storek, B, Reinhardt, M, Wang, C, Janssen, WG, Harder, NM, Banck, MS *et al*. (2008). Sensory neuron targeting by self-complementary AAV8 via lumbar puncture for chronic pain. *Proc Natl Acad Sci USA* **105**: 1055–1060.
10 Towne, C, Pertin, M, Beggah, AT, Aebischer, P and Decosterd, I (2009). Recombinant adeno-associated virus serotype 6 (rAAV2/6)-mediated gene transfer to nociceptive neurons through different routes of delivery. *Mol Pain* **5**: 52.
11 Mason, MR, Ehlert, EM, Eggers, R, Pool, CW, Hermening, S, Huseinovic, A *et al*. (2010). Comparison of AAV serotypes for gene delivery to dorsal root ganglion neurons. *Mol Ther* **18**: 715–724.
12 Zheng, H, Qiao, C, Wang, CH, Li, J, Li, J, Yuan, Z *et al*. (2010). Efficient retrograde transport of adeno-associated virus type 8 to spinal cord and dorsal root ganglion after vector delivery in muscle. *Hum Gene Ther* **21**: 87–97.
13 White, E, Bienemann, A, Sena-Esteves, M, Taylor, H, Bunnun, C, Castrique, E *et al*. (2011). Evaluation and optimization of the administration of recombinant adeno-associated viral vectors (serotypes 2/1, 2/2, 2/rh8, 2/9, and 2/rh10) by convection-enhanced delivery to the striatum. *Hum Gene Ther* **22**: 237–251.
14 Sondhi, D, Hackett, NR, Peterson, DA, Stratton, J, Baad, M, Travis, KM *et al*. (2007). Enhanced survival of the LINCL mouse following CLN2 gene transfer using the rh.10 rhesus macaque-derived adeno-associated virus vector. *Mol Ther* **15**: 481–491.
15 Zhang, H, Yang, B, Mu, X, Ahmed, SS, Su, Q, He, R *et al*. (2011). Several rAAV vectors efficiently cross the blood-brain barrier and transduce neurons and astrocytes in the neonatal mouse central nervous system. *Mol Ther* **19**: 1440–1448.
16 Hu, C, Busuttil, RW and Lipshutz, GS (2010). RH10 provides superior transgene expression in mice when compared with natural AAV serotypes for neonatal gene therapy. *J Gene Med* **12**: 766–778.
17 Federici, T, Taub, JS, Baum, GR, Gray, SJ, Grieger, JC, Matthews, KA *et al*. (2012). Robust spinal motor neuron transduction following intrathecal delivery of AAV9 in pigs. *Gene Ther* **19**: 852–859.
18 Snyder, BR, Gray, SJ, Quach, ET, Huang, JW, Leung, CH, Samulski, RJ *et al*. (2011). Comparison of adeno-associated viral vector serotypes for spinal cord and motor neuron gene delivery. *Hum Gene Ther* **22**: 1129–1135.
19 Samaranch, L, Salegio, EA, San Sebastian, W, Kells, AP, Bringas, JR, Forsayeth, J *et al*. (2013). Strong cortical and spinal cord transduction after AAV7 and AAV9 delivery into the cerebrospinal fluid of nonhuman primates. *Hum Gene Ther* **24**: 526–532.
20 Gray, SJ, Nagabhushan Kalburgi, S, McCown, TJ and Jude Samulski, R (2013). Global CNS gene delivery and evasion of anti-AAV-neutralizing antibodies by intrathecal AAV administration in non-human primates. *Gene Ther* **20**: 450–459.
21 Kennedy, JM and Zochodne, DW (2000). The regenerative deficit of peripheral nerves in experimental diabetes: its extent, timing and possible mechanisms. *Brain* **123** (Pt 10): 2118–2129.
22 Homs, J, Ariza, L, Pagès, G, Verdú, E, Casals, L, Udina, E *et al*. (2011). Comparative study of peripheral neuropathy and nerve regeneration in NOD and ICR diabetic mice. *J Peripher Nerv Syst* **16**: 213–227.
23 Craner, MJ, Klein, JP, Black, JA and Waxman, SG (2002). Preferential expression of IGF-I in small DRG neurons and down-regulation following injury. *Neuroreport* **13**: 1649–1652.
24 Franco, LM, Sun, B, Yang, X, Bird, A, Zhang, H, Schneider, A *et al*. (2005). Evasion of immune responses to introduced human acid alpha-glucosidase by liver-restricted expression in glycogen storage disease type II. *Mol Ther* **12**: 876–884.
25 Wang, L, Dobrzynski, E, Schlachterman, A, Cao, O and Herzog, RW (2005). Systemic protein delivery by muscle-gene transfer is limited by a local immune response. *Blood* **105**: 4226–4234.
26 Bevan, AK, Hutchinson, KR, Foust, KD, Braun, L, McGovern, VL, Schmelzer, L *et al*. (2010). Early heart failure in the SMNDelta7 model of spinal muscular atrophy and correction by postnatal scAAV9-SMN delivery. *Hum Mol Genet* **19**: 3895–3905.
27 Foust, KD, Wang, X, McGovern, VL, Braun, L, Bevan, AK, Haidet, AM *et al*. (2010). Rescue of the spinal muscular atrophy phenotype in a mouse model by early postnatal delivery of SMN. *Nat Biotechnol* **28**: 271–274.
28 Dominguez, E, Marais, T, Chatauret, N, Benkhelifa-Ziyyat, S, Duque, S, Ravassard, P *et al*. (2011). Intravenous scAAV9 delivery of a codon-optimized SMN1 sequence rescues SMA mice. *Hum Mol Genet* **20**: 681–693.
29 Towne, C, Schneider, BL, Kieran, D, Redmond, DE Jr and Aebischer, P (2010). Efficient transduction of non-human primate motor neurons after intramuscular delivery of recombinant AAV serotype 6. *Gene Ther* **17**: 141–146.
30 Duque, S, Joussemet, B, Riviere, C, Marais, T, Dubreil, L, Douar, AM *et al*. (2009). Intravenous administration of self-complementary AAV9 enables transgene delivery to adult motor neurons. *Mol Ther* **17**: 1187–1196.
31 Bevan, AK, Duque, S, Foust, KD, Morales, PR, Braun, L, Schmelzer, L *et al*. (2011). Systemic gene delivery in large species for targeting spinal cord, brain, and peripheral tissues for pediatric disorders. *Mol Ther* **19**: 1971–1980.
32 Samaranch, L, Salegio, EA, San Sebastian, W, Kells, AP, Foust, KD, Bringas, JR *et al*. (2012). Adeno-associated virus serotype 9 transduction in the central nervous system of nonhuman primates. *Hum Gene Ther* **23**: 382–389.
33 Foust, KD, Nurre, E, Montgomery, CL, Hernandez, A, Chan, CM and Kaspar, BK (2009). Intravascular AAV9 preferentially targets neonatal neurons and adult astrocytes. *Nat Biotechnol* **27**: 59–65.
34 Boutin, S, Monteilhet, V, Veron, P, Leborgne, C, Benveniste, O, Montus, MF *et al*. (2010). Prevalence of serum IgG and neutralizing factors against adeno-associated virus (AAV) types 1, 2, 5, 6, 8, and 9 in the healthy population: implications for gene therapy using AAV vectors. *Hum Gene Ther* **21**: 704–712.
35 Fukuda, R, Hirota, K, Fan, F, Jung, YD, Ellis, LM and Semenza, GL (2002). Insulin-like growth factor 1 induces hypoxia-inducible factor 1-mediated vascular endothelial growth factor expression, which is dependent on MAP kinase and phosphatidylinositol 3-kinase signaling in colon cancer cells. *J Biol Chem* **277**: 38205–38211.
36 Mason, JL, Xuan, S, Dragatsis, I, Efstratiadis, A and Goldman, JE (2003). Insulin-like growth factor (IGF) signaling through type 1 IGF receptor plays an important role in remyelination. *J Neurosci* **23**: 7710–7718.
37 Delaney, CL, Russell, JW, Cheng, HL and Feldman, EL (2001). Insulin-like growth factor-I and over-expression of Bcl-xL prevent glucose-mediated apoptosis in Schwann cells. *J Neuropathol Exp Neurol* **60**: 147–160.
38 Brussee, V, Cunningham, FA and Zochodne, DW (2004). Direct insulin signaling of neurons reverses diabetic neuropathy. *Diabetes* **53**: 1824–1830.
39 Leinninger, GM, Vincent, AM and Feldman, EL (2004). The role of growth factors in diabetic peripheral neuropathy. *J Peripher Nerv Syst* **9**: 26–53.
40 Apfel, SC, Schwartz, S, Adornato, BT, Freeman, R, Biton, V, Rendell, M *et al*. (2000). Efficacy and safety of recombinant human nerve growth factor in patients with diabetic polyneuropathy: a randomized controlled trial. rhNGF Clinical Investigator Group. *JAMA* **284**: 2215–2221.
41 Isner, JM, Ropper, A and Hirst, K (2001). VEGF gene transfer for diabetic neuropathy. *Hum Gene Ther* **12**: 1593–1594.
42 Wellmer, A, Misra, VP, Sharief, MK, Kopelman, PG and Anand, P (2001). A double-blind placebo-controlled clinical trial of recombinant human brain-derived neurotrophic factor (rhBDNF) in diabetic polyneuropathy. *J Peripher Nerv Syst* **6**: 204–210.
43 Ekberg, K, Brismar, T, Johansson, BL, Lindström, P, Juntti-Berggren, L, Norrby, A *et al*. (2007). C-Peptide replacement therapy and sensory nerve function in type 1 diabetic neuropathy. *Diabetes Care* **30**: 71–76.
44 Li, H, Malani, N, Hamilton, SR, Schlachterman, A, Bussadori, G, Edmonson, SE *et al*. (2011). Assessing the potential for AAV vector genotoxicity in a murine model. *Blood* **117**: 3311–3319.
45 Sharma, A and Thomas, P (1987). Animal model: pathology and pathophysiology. In: Dyck, P, Thomas, P, Asbury, A, Winegrad, A and Porte, D Jr (eds). *Diabetic Neuropathy, 1st ed*. Saunders: Philadelphia. pp. 237–252.
46 Wright, A and Nukada, H (1994). Sciatic nerve morphology and morphometry in mature rats with streptozocin-induced diabetes. *Acta Neuropathol* **88**: 571–578.
47 Mizisin, AP, Nelson, RW, Sturges, BK, Vernau, KM, Lecouteur, RA, Williams, DC *et al*. (2007). Comparable myelinated nerve pathology in feline and human diabetes mellitus. *Acta Neuropathol* **113**: 431–442.
48 Zolotukhin, S, Byrne, BJ, Mason, E, Zolotukhin, I, Potter, M, Chesnut, K *et al*. (1999). Recombinant adeno-associated virus purification using novel methods improves infectious titer and yield. *Gene Ther* **6**: 973–985.
49 Xiao, X, Li, J and Samulski, RJ (1998). Production of high-titer recombinant adeno-associated virus vectors in the absence of helper adenovirus. *J Virol* **72**: 2224–2232.
50 Pfaffl, MW (2001). A new mathematical model for relative quantification in real-time RT-PCR. *Nucleic Acids Res* **29**: e45.

Supplementary Information accompanies this paper on the *Molecular Therapy—Methods & Clinical Development* website (http://www.nature.com/mtm)